Flight Cryogenic System for the Micro-X Sounding Rocket

P. Wikus[1], J. M. Rutherford[1], S.N. Trowbridge[1], D. McCammon[4], J. S. Adams[2], S. R. Bandler[2], R. Das[1], W. B. Doriese[3], M. E. Eckart[2], E. Figueroa-Feliciano[1], R. L. Kelley[2], C. A. Kilbourne[2], S. W. Leman[1], F.S. Porter[2] and K. Sato[1]

[1] Massachusetts Institute of Technology, Cambridge, MA 02139
[2] NASA Goddard Space Flight Center, Greenbelt, MD 20771
[3] National Institute of Standards and Technology, Boulder, CO 80305
[4] University of Wisconsin, Madison, WI 53706

ABSTRACT

The Micro-X Imaging X-ray Spectrometer is a sounding rocket payload slated for launch in 2011. An array of transition edge sensors will be used to obtain high resolution X-ray spectra of astronomical sources.

An Adiabatic Demagnetization Refrigerator (ADR) forms the heart of the instrument's cryogenic system. It consists of a Ferric Ammonium Alum (FAA) salt pill in the bore of a low current 4 T superconducting magnet. The detector array is accommodated inside a magnesium housing which is thermally connected to the FAA salt. A bath of superfluid helium functions as a heat sink for the ADR. The helium tank is suspended inside a lightweight aluminum vacuum vessel by a set of reentrant G10 thrust tubes.

The cryogenic system has been designed to withstand the extreme structural loads encountered in rocket flight, while at the same time providing hold-times sufficiently long to facilitate convenient operation during the launch campaign. Due to the short duration of a sounding rocket flight, the thermal recovery time constant of the cold mass had to be kept on the order of only a few seconds. In addition, special attention has been paid to minimizing the heating of the cold stage due to the dissipation of vibration originating from the rocket motor.

The assembly of the Micro-X cryogenic system has been completed, and performance tests have been carried out. The design of the Micro-X cryogenic system and the results of the performance tests are presented here-in.

INTRODUCTION

The use of small calorimeters operated at cryogenic temperatures as single particle detectors was first proposed by Niinikoski in 1975[1]. In 1984, Moseley et al.[2] suggested using cryogenic microcalorimeters as high resolution X-ray spectrometers. Since then, the technology readiness of entire arrays of X-ray microcalorimeters has advanced rapidly, leading to the development of the XQC sounding rocket instrument[3] and the XRS instrument on the Japanese-US X-ray astronomy satellites Astro-E[4] and Astro-E2[5]. The design of these instruments relied on semiconductor thermistors, i.e. high impedance sensors, to determine the temperature of the microcalorimeters.

Cryocoolers 16, edited by S.D. Miller and R.G. Ross, Jr.

Transition Edge Sensor (TES) Microcalorimeters

To measure the temperature rise caused by an incident photon, TES microcalorimeters make use of the steep resistance (R) vs. temperature (T) characteristic of a superconducting film that is biased in its transition. The logarithmic sensitivity, defined as $\alpha = T/R \cdot dR/dT_{(I)}$, of TESs can be more than an order of magnitude higher than for semiconductor thermistors, which leads to the exquisite energy resolution of TES-based X-ray microcalorimeters. These detectors have demonstrated energy resolutions as good as 2 eV Full Width at Half Max (FWHM) at 6 keV[6]. TESs are low impedance devices, and are commonly read out with Superconducting Quantum Interference Devices (SQUIDs), which provide good impedance matching to conventional room temperature electronics. Arrays of microcalorimeter pixels have been successfully readout using SQUID time division multiplexers[7].

Figure 1 shows the detector front-end assembly (FEA) of the Micro-X instrument, whose cryogenic system is discussed in this work. The TES array, consisting of 128 active pixels, is located in the center of the assembly. It is flanked by shunt resistors (for the TES bias circuit) and SQUID chips, the latter of which provide the first two cold amplification stages and the multiplexing capability. The entire assembly is coupled to the cold stage of an ADR. To achieve the targeted energy resolution of < 4 eV FWHM at 6 keV – using TESs with a transition temperature of approximately 90 mK – we plan to cool the assembly to approximately 50 mK. For the TES detector arrays that we have fabricated for initial system tests, which have a higher transition temperature (170 mK) and exhibit energy resolutions of ~6-9 eV FWHM at 6 keV, higher temperatures are sufficient (approximately ~100 mK). The energy resolution of a TES microcalorimeter is also influenced by the temperature stability, which needs to be stable to the order of 1 μK peak-to-peak to achieve the targeted energy resolution.

The Micro-X Imaging X-Ray Spectrometer

The Micro-X Imaging X-ray Spectrometer[8], in short Micro-X, will be the first instrument to use TES microcalorimeters in a space-borne observation. It will obtain the first high-resolution X-ray spectrum of a spatially extended source, and serve as a technology demonstration for future orbiting X-ray telescopes using TES technology.

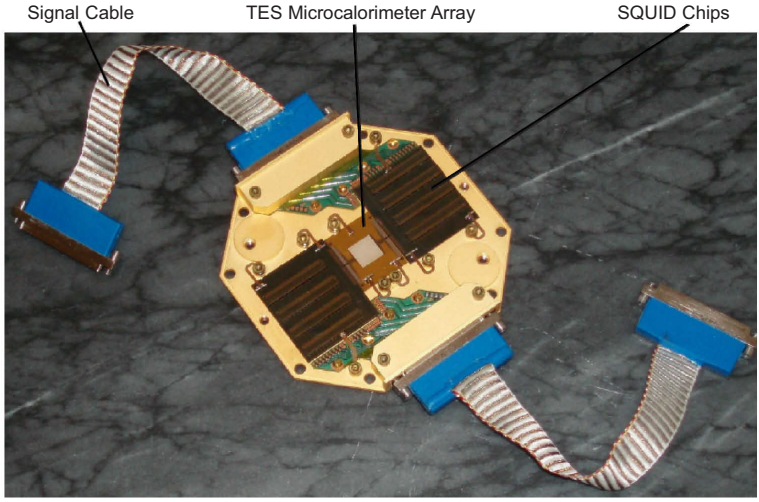

Figure 1. The Front End Assembly (FEA) of the Micro-X sounding rocket telescope. The TES array and SQUID chips are kinematically mounted on a gold-plated magnesium cold plate, which is coupled to the cold stage of an ADR. The two signal cables connect the FEA to SQUID series arrays which are mounted on the LHe stage of the cryostat. The FEA measures approximately 75 mm from side to side.

The Micro-X sounding rocket payload, shown in Figure 2, will be launched on a ballistic trajectory by a sounding rocket from the White Sands Missile Range in New Mexico. The first flight of the instrument is planned for 2011, and will likely target the Puppis A supernova remnant[9]. The observation will be performed above an altitude of 160 km, and last approximately 300 seconds. Micro-X has successfully passed the design review in February 2010; the integration of the flight hardware is currently underway.

Due to the short duration of the flight, the microcalorimeter array has to be cooled to its operating temperature on the ground. The temperature of the array is expected to rise during ascent, when heat is deposited in the cold stage due to damping of the mechanical vibrations originating from the rocket motors. This temperature rise has to be kept small to ensure that the operating temperature can be achieved a few seconds after burnout. In addition, operational constraints call for a hold time at base temperature of several hours; the liquid helium (LHe) reservoir, which serves as a heat sink and intercept for the ADR, should have a hold time in excess of 12 hours. Since TESs and SQUIDs are very susceptible to magnetic fields, a magnetic shield is required which attenuates the stray fields of the ADR magnet by several orders of magnitude.

CRYOGENIC SYSTEM OVERVIEW

The design of the cryogenic system for Micro-X is largely based on the very successful design of the XQC sounding rocket cryostat[10]. The ADR consisting of a superconducting magnet, a heat switch, and the cold stage with the salt pill – is accommodated in the central bore of a cylindrical helium tank. The helium tank is suspended from the inside of the vacuum vessel by a set of reentrant G10 thrust tubes. Vapor-cooled thermal shields surround the helium can.

The most important changes from the XQC design were the implementation of a magnetic shield for the detectors, which led to a longer cold stage and a change in the Kevlar suspension of the cold stage. In addition, changes to the layout of the LHe cold space were necessary to accommodate the LHe stage SQUID electronics. The inner thermal shield was extended around the aft section of the LHe stage. The dewar for Micro-X is slightly larger than the one for XQC.

A cross-section of the Micro-X flight dewar is shown in the schematic in Fig. 3, and a photo of the flight hardware is shown in Fig. 4. The cryogenic system has a mass of 31.5 kg, and is 400 mm in diameter and 394 mm in height.

THE LIQUID HELIUM STAGE

The LHe stage serves as a heat sink for the ADR. The reservoir has a volume of 6.5 liters. In the first performance test, the heat load on the helium bath was measured at 85 mW; after a complete fill, a subsequent pump-down and some time for thermalization, approximately 3 liters of LHe remain in the tank. The hold time below a temperature of 1.5 K amounts to 22 hours. The coldest temperature measured at the LHe stage was 1.3 K, and was achieved with a fairly short pump-line and a 65 m^3/h pump.

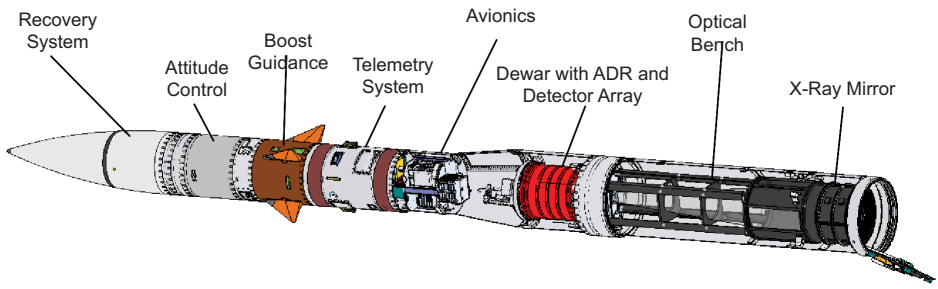

Figure 2. The Micro-X sounding rocket payload. Photons enter the instrument from the right side through the X-ray mirror, which focuses them onto the TES microcalorimeter array. The focal length is 2100 mm. The FEA with the detector array − shown in Fig. 1 and Fig. 4 on the next page − is located inside the dewar and is cooled by an ADR. The length of the payload amounts to approximately 7 m.

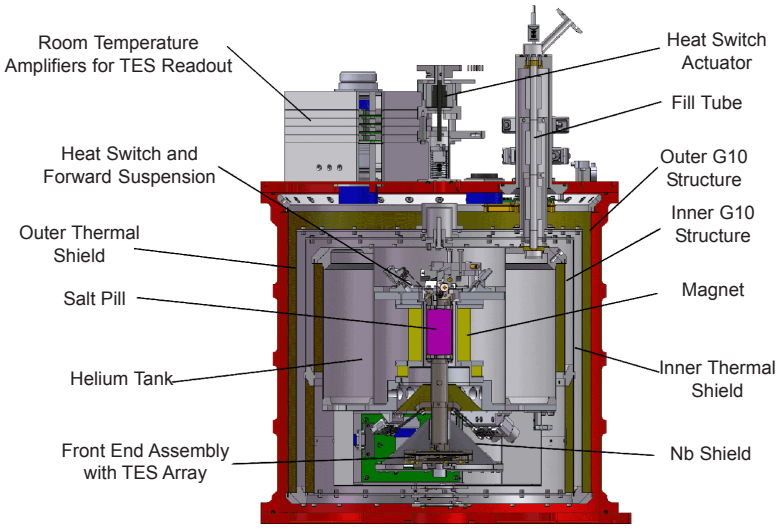

Figure 3. Cross-section through the CAD model of the Micro-X flight dewar. X-rays enter the dewar through a set of infrared filters from the bottom end. The vacuum space is sealed with a gate valve, which is opened in space to allow the passage of X-rays.

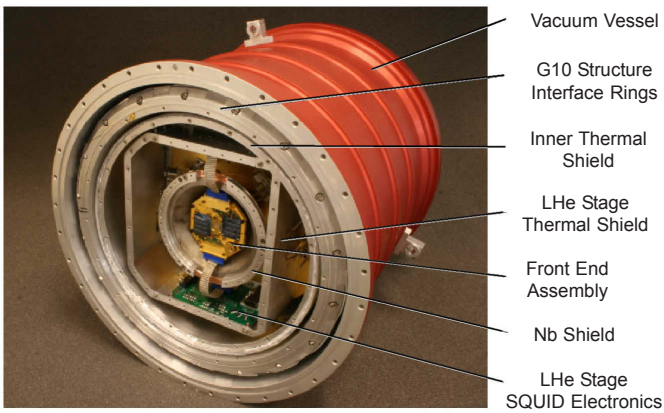

Figure 4. The flight hardware of the cryogenic system, with the aft thermal shield lids and the aft vacuum flange removed. The FEA, also shown in Fig. 1, is mounted on the salt pill and sits in the center of the magnetic shield. It is surrounded by several thermal shields.

The LHe tank is a welded aluminum structure with two openings, one for a level gauge, and the other for the fill tube. Both are connected to the helium tank with indium seals. The fill tube serves both as a port to fill cryogens into the tank, and as an exhaust line for the boil-off vapors. It consists of four stainless steel tube sections, which are interconnected with flexible bellows. These bellows compensate mismatches in the thermal expansion coefficients of the various construction materials, and cause turbulence in the gas leaving the helium can. This is necessary to improve the heat transfer between the gas and the wall of the fill tube for cooling two thermal shields which are heat sunk to the outside of the fill tube.

On the launch rail, a pump will be used to maintain a low pressure above the bath in the helium can. Just before launch, a valve seals off the helium can for the rocket's ascent through the atmosphere until payload separation, which occurs 68 seconds into the flight at an altitude of approximately 90 km. At that altitude, the residual atmospheric pressure is low enough to open the valve again and let the vacuum of space pump on the helium bath.

A disk made from sintered stainless steel (which was supplied by Mott Corporation, has a pore size of 1 μm, and a thickness of 1.6 mm) is located in the cold end of the fill tube. This disk has a hole in its center to provide a low impedance passage for the initial pump-down. For flight, the hole is plugged to prevent LHe from sloshing into the warm region of the fill line.

THE VACUUM VESSEL AND INTERNAL SUPPORT STRUCTURE

The helium tank is suspended from the inside wall of the vacuum vessel by G10 thrust tubes, and is surrounded by two thermal shields. The G10 tubes have a wall thickness of 0.5 mm. The outer G10 support structure, visible in Fig. 3, consists of a single G10 tube with a diameter of 350 mm and a length of 334 mm. The inner G10 support structure consists of two G10 tubes (with diameters of 309 and 299 mm respectively), which are joined by an aluminum ring to provide a mounting point for the split inner thermal shield. The G10 tubes were custom-made by Stevens Products. To provide suitable mechanical interfaces for bolt connections at both ends of the G10 tubes, they were epoxied into grooves in aluminum rings with Armstrong A12 epoxy. The grooves are 0.25 mm wider than the wall thickness of the G10 tubes. Pull tests proved that the strength of the glue joints exceeds the strength of the G10 tubes.

The cables carrying the signals for the detector readout between the LHe stage and the room temperature flange are routed along the G10 tubes. A total of 80 twisted pairs, made from 0.09 mm diameter Alloy 30 wire, were woven into two aramid looms by Tekdata Interconnections Ltd.

Two vapor cooled thermal shields surround the helium can; both are heat sunk to the fill tube. During performance testing, the shield temperatures were measured at 72 K and 219 K, higher than expected. It is assumed that the shield temperatures – and the heat load on the helium bath – can be lowered by improving the thermal contact between the shields and the fill tube. All G10 tubes and thermal shields are wrapped in 20-sheet CoolCat 2NW multilayer insulation from RUAG Space GmbH. The thermal shields were welded from 0.5 and 1 mm thin Al sheets.

The vacuum vessel consists of three aluminum parts. The cylindrical wall has been machined from a single piece, and is closed off at both ends with flat flanges. The room-temperature preamplifiers for the detector read out and the actuator for the heat switch are mounted to the top flange of the dewar.

Fig. 5 shows the various stages of the assembly of the Micro-X flight dewar.

THE ADIABATIC DEMAGNETIZATION REFRIGERATOR

The heart of the cryogenic system is an ADR which provides cooling to the detector array. The paramagnetic refrigerant is located in the bore of a superconducting solenoid. A mechanical heat switch is located at one end of the salt pill, the Front End Assembly (FEA) with the TES detectors on the other. The cold stage is suspended with Kevlar strings.

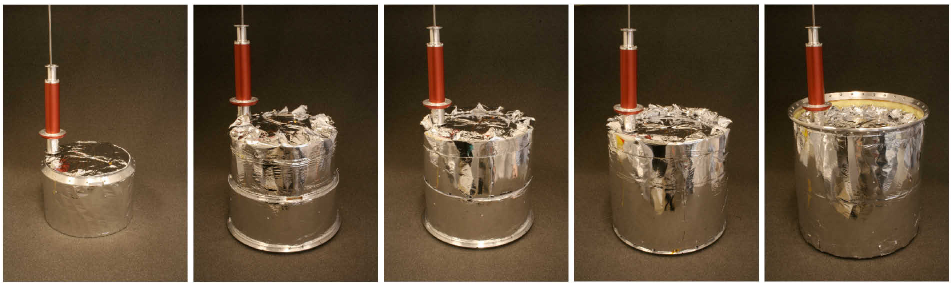

(a) (b) (c) (d) (e)

Figure 5. The Micro-X flight dewar can be likened to a “Russian Doll”, with the helium can in the center. From left to right: (a) Helium Tank (b) Inner G10 Structure (c) Inner Thermal Shield (d) Outer Thermal Shield (e) Outer G10 Structure. The vacuum cover for the helium fill tube is visible on the top.

The Superconducting Magnet and Current Leads

A custom-made multifilament NbTi/Cu solenoid magnet was purchased from Cryomagnetics, Inc. At the full operating current of 9.7 A, the maximum field density in the center of the bore is 4 T. Due to this low current design, which eases the requirements on the power supply and the current leads, the inductance of the magnet amounts to 22 H. The magnet is located in the vacuum space of the dewar, i.e. cooling is provided through conduction only, and is protected by electronic circuitry.

Current is supplied to the magnet through four high-temperature BSSCO superconductor tapes (to provide redundancy, two tapes each for supply and return were installed), which were glued to the innermost G10 tube, and operate between the temperature of the helium can and the inner thermal shield. For the section of the current leads operating at higher temperatures, Alloy 30 wire was chosen. This copper alloy consists of 98 percent copper and 2 percent Nickel. It has a low Residual Resistivity Ratio (RRR) of 1.5[11], and is thus well suited to prevent thermal runaway of the current leads.

To allow for easy removal of the magnet from the dewar for maintenance, high current connectors have been installed at the LHe stage where the current leads can be disconnected. The voltage drop in these high current connectors (SP4N and BL4N from Multi-Contact AG) is on the order of 300 μV at a current of 4.25 A and a temperature of approximately 1.7 K.

The Cold Stage, Suspension and Heat Switch

The cold stage mainly consists of the salt pill, which contains the paramagnetic refrigerant, and the FEA. Ferric Ammonium Alum (FAA) was used for the construction of the salt pill. 75 grams of FAA have been grown around a bundle of 150 annealed gold wires with a diameter of 0.2 mm each. The FAA salt is enclosed in a welded stainless steel housing. The gold wires were brazed to two copper heat busses, one at each end of the salt pill. To protect the copper heat busses and the brazed joints from the corrosive salt, they were gold plated and painted with Stycast 1250 FT.

The salt pill is shown in Fig. 6. In the performance tests, a base temperature of less than 45 mK (which is the lowest temperature the cold stage thermometer is calibrated to) was achieved. At the same time, an abnormally low thermal conductance of 0.3 μW/mK between the heat bus and the paramagnetic salt was measured at a temperature of 60 mK, and 0.6 μW/mK at 100 mK; values typically achieved with salt pills of similar design are around 1.5 μW/mK at 60 mK. This is attributed to irregularities during either the gold plating or the brazing processes, and mandates the construction of a new salt pill if operation at 50 mK is desired. The current salt pill is well suitable for extended operation at higher FEA temperatures above 100 mK, however.

The heat switch is a simple mechanical clamp which is actuated by pulling on a Kevlar string threaded through the thermal shields from the LHe stage to the top flange of the vacuum vessel, where the actuation mechanism is located. The conductance of the heat switch was measured to be

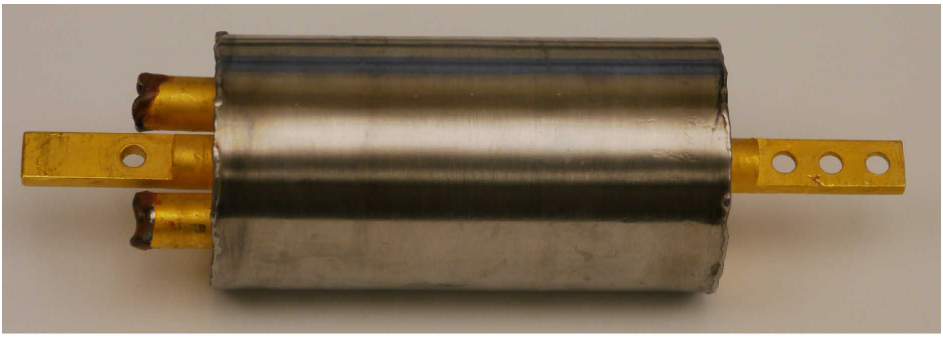

Figure 6. The paramagnetic FAA refrigerant is hermetically sealed in a welded stainless steel can. The two gold plated copper heat busses at each end of the salt pill are the thermal interfaces for the detector assembly and the heat switch.

0.63 μW/mK at a temperature of 1.63 K, which is comparable to a prior designs[12] and allows for rapid thermalization of the salt during a magnet cycle.

The entire cold stage has a mass of 255 g and is suspended from the helium tank with seven 4560 denier Kevlar-49 loops. Six of the loops kinematically constrain the six degrees of freedom of the suspended mass, and one applies a constant pre-tensioning force through a spring. The suspension was designed to withstand accelerations in excess of 200 *g*, and to have a high resonant frequency of a few hundred Hz. This high resonant frequency is required to minimize heating of the suspended mass due to the high vibrations during launch[13]. The total heat load from the Kevlar suspension system has been measured to amount to 0.88 μW. Care was taken to keep the thermal time constants of the assembly low by refraining from the use of materials with low thermal conductivity or high specific heat. The stainless steel housing of the salt pill is thermally coupled to one of the heat busses with Cu heat sinking strips.

Signals from the detector array inside the FEA are routed to the LHe stage electronics through two woven aramid looms, each containing 43 twisted pairs, which were made from 0.05 mm thin superconducting NbTi wire with CuNi cladding to keep the heat load on the cold stage low.

The Magnetic Shield

Since TESs and SQUIDs are sensitive to magnetic fields, the detector assembly has to be shielded from fields generated by the superconducting magnet; static fields in the region of the detector array must not exceed 1 μT, and time varying fields need to be below approximately 3 pT sqrt(Hz). A magnetic shield consisting of three stages has been implemented; the first stage is a bucking coil wired in series with the main coil of the ADR magnet and reduces the stray field of the main coil in the aft region of the magnet. The second stage is a shield plate made from a high permeability material; the third stage is a superconducting can surrounding the detector assembly. The first design of the magnetic shield has been described in detail in the work by Wilkus, et.al.[14]. After some minor changes to that design, mainly concerning the material selection for the high permeability shield (Ultra Low Carbon Steel (UCLS) instead of Cryoperm) and the geometry of the superconducting and high-permeability parts, the design was implemented and tested.

The residual field of the magnet was measured at the location of the detector array inside the magnetic shield, in the direction perpendicular to the TES array. The ratio between the field change in the magnet and the corresponding field change at the location of the detector array is $2 \cdot 10^{-5}$, which is more than 3 orders of magnitude higher than what axially symmetric finite element simulations predicted. Additional finite element simulations, which were extended to three dimensions, revealed that the initial shield design is extremely susceptible to even a small misalignment which breaks axial symmetry, and provides only small field attenuation (approximately by a factor 5) in the direction which is parallel to the TES array. The measured attenuation puts the Micro-X magnetic shield design on the verge of being acceptable, and more accurate field measurements with SQUIDs have to be performed.

CONTROL ELECTRONICS

The cryogenic system is controlled by electronics copied from the XQC payload[3,10]. This system provides readout for important housekeeping values, such as the LHe level and the temperature of the LHe stage. In addition, it controls the temperature of the ADR cold stage by controlling the *voltage* across the terminals of the superconducting magnet. A schematic of the ADR control electronics is shown in Fig 7.

The control system reads two germanium resistance thermometers; only one is used for temperature control, the other serves as a monitor. For simplicity, only one thermometer readout is shown in Fig 7. The resistance of the thermometers is measured with a lock-in amplifier in a nulling loop circuit. A sine generator operating at a frequency of 17.58 Hz (to avoid any low beat frequencies with 60 Hz pickup) is used to create a fixed-amplitude sine wave (a). This signal is passed through a 200 pF capacitor (b), which has a high complex impedance at the low operating frequency, and converts the 5 V sine wave into a small cosine drive current (1.6 nA) that is passed

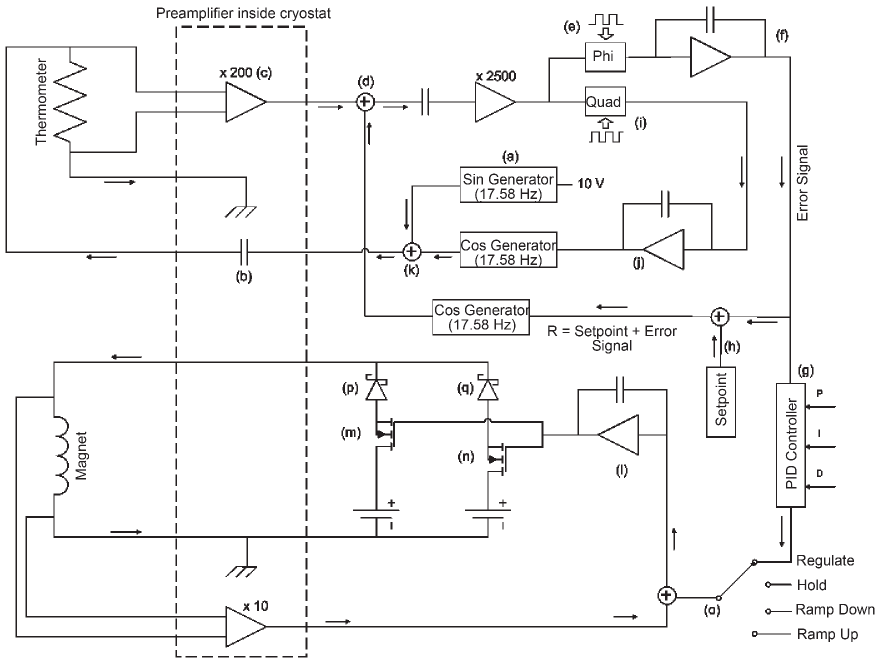

Figure 7. Simplified schematic of the control electronics for the ADR. Only one thermometer readout channel is shown.

through the resistance thermometer. The resulting voltage drop is measured, and pre-amplified by a factor of 200 inside the cryostat (c).

The room temperature part of the thermometer readout consists of two closed loops; the first one measures the difference between the actual resistance of the thermometer and the predefined set-point, providing the error signal. The amplified voltage signal across the resistance thermometer is summed with a nulling signal (d). The difference, a very small signal, is amplified by a factor of 2500 and multiplied by a square wave in phase with the current drive (e). The output of this phase detector is integrated (f). As long as any inphase signal is present at the error amplifier output, the integrator output will continue to increase (or decrease, if the signal is 180° out of phase with the reference). This output is intended to be the temperature error signal and therefore remains near zero in normal operation. It is sent to the input of the PID temperature controller (g) and is also added to a fixed DC voltage representing the resistance of the thermometer at the temperature setpoint (h). The setpoint plus error voltage is converted to a cosine wave and becomes the nulling signal at the amplifier input.

A second loop, called the quadrature loop, compensates for the phase shift of the excitation signal due to stray capacitance in the thermometer wiring. This phase shift would reduce the inphase excitation current to the thermometer and change the resistance reading. The presence of an unnulled quadrature signal at the input to the phase detector would also produce an unacceptable ripple in the error signal. This is avoided with a second phase detector operated at 90° to the first (i), feeding a second integrator (j). The output of this integrator is converted to a quadrature phase component that is added to the drive current (k). This increases until the quadrature phase signal across the thermometer resistance disappears. This added drive current component is then providing all the current flowing through shunt capacitances, and the current through the thermometer is entire inphase and at its original amplitude, so no correction for phase shift is required.

The PID controller, which is fed with the temperature error signal, outputs a signal proportional to the desired voltage across the terminals of the superconducting magnet. This voltage is combined with the actual voltage across the magnet to provide a voltage error signal, which is integrated (l). The output of the integrator controls two redundant power MOSFET supplies (m, n).

"Too cold" error signals result in a positive voltage that ramps up the magnetic field and warms the paramagnetic salt. "Too hot" does the opposite. To perform functions other than temperature control, such as ramping up, ramping down, or holding the current constant, the output of the PID controller is replaced with constant voltages (o) - positive to ramp up the magnet current, negative to ramp down, and zero to hold at constant current, since for a superconducting magnet $dI/dt \sim V$. Controlling the magnet voltage rather than current allows the magnet inductance to filter power supply noise, and the simple control provided by this circuit can regulate the temperature to better than 100 nK rms on a 1 Hz bandwidth. The current to the magnet is passed through two Schottky diodes (p, q) which help to evenly distribute the load between the two supplies at high current, and isolate the two supplies in case one fails shorted.

FUTURE WORK

The first performance tests of the flight hardware of the Micro-X cryogenic system yielded very promising results and mostly met the project's requirements for the operation of a 9.5 eV resolution TES array. To provide a suitable environment for a TES array with an energy resolution below 4 eV, the following improvements will be made:

- A new salt pill with an improved thermal contact between the salt and the heat bus will allow for operation at lower temperatures, and improve the hold time of the system, since the salt can be kept at a higher temperature for a given FEA temperature.
- Thermal coupling of the shields to the fill tube will be improved. This will lower the heat load on the helium stage and improve the hold time, and lower the thermal shield temperatures. Lower shield temperatures are beneficial as the infrared filters, which are mounted on the thermal shields, will run at a correspondingly lower temperature. This reduces shot noise and lowers the thermal loading of the microcalorimeters.
- Following more accurate magnetic field measurements with SQUIDs, a redesign of the magnetic shield may be necessary to allow for operation at an energy resolution below 4 eV. Options include a change of the geometry of the superconducting can, and a high permeability liner inside the Nb can.

ACKNOWLEDGMENTS

The Micro-X project is funded through NASA grant NNX10AE25G. Kosuke Sato is supported by a JSPS fellowship for research abroad. The authors thank Bruker HTS GmbH and American Magnetics Inc. for supplying samples of superconducting materials for the construction of the MicroX cryostat, DuPont for providing samples of Kevlar yarn for the construction of the cold stage suspension, and the Mott Corporation for providing sintered stainless steel disks.

REFERENCES

1. Niinikoski, T.O., "Cosmic-Ray Disturbances in Thermometry and Refrigeration," *Liquid and Solid Helium* (1975), pp. 145-147.
2. Moseley, S.H., Mather, J.C., and McCammon, D., "Thermal Detectors as Xray Spectrometers," *J. Appl. Phys.* 56 (1984), pp. 1257-1262.
3. McCammon, D., et al., "A Sounding Rocket Payload for X-ray Astronomy Employing High-Resolution Microcalorimeters," *Nucl. Instrum. Methods Phys. Res.,* Sect. A 370 (1996), pp. 266-268.
4. Kelley, R.L., et al., "The Microcalorimeter Spectrometer on the ASTRO-E X-ray Observatory," *Nucl. Instr. and Meth.* 444 (2000), pp. 170-174.
5. Kelley, R.L., et al., "The Suzaku High Resolution X-Ray Spectrometer," *Publications of the Astronomical Society of Japan* 59 (2007), pp. 77-112.
6. Bandler, S. R., et al., "Performance of TES X-ray Microcalorimeters with a Novel Absorber Design," *J. of Low Temp. Phys.* 151 (2008), pp. 400-405.

7. Doriese, W.B., et al., “Progress toward Kilopixel Arrays: 3.8 eV Microcalorimeter Resolution in 8Channel SQUID Multiplexer," *NIMPA* V559 (2006), p. 808-810.

8. Wikus, P., et al., “Micro-X, the High Resolution Sounding Rocket X-ray Imaging Spectrometer," *Proceedings of the 19th ESA Symposium on European Sounding Rocket and Balloon Programmes and Related Research*, ESA-SP 671 (2009), pp. 573-577.

9. Figueroa-Feliciano, E., et al., “New Science Case for the Micro-X High Energy Resolution Microcalorimeter X-ray Imaging Rocket," *Proceedings of the 13th International Workshop on Low Temperature Detectors*, AIPCP 1185 (2009), pp. 426-429.

10. Porter, F. S., et al.,”The XQC microcalorimeter sounding rocket: a stable LTD platform 30 seconds after rocket motor burnout," *Nuclear Instruments and Methods* 444 (2000), pp. 220-223.

11. Porter, F.S., and Adams, J., NASA Goddard Space Flight Center, private communication, May 2009.

12. Pobell, F., *Matter and Methods at Low Temperatures*, 2nd edition, Springer, Berlin (1995), p. 75.

13. Wikus, P., et al., “The Adiabatic Demagnetization Refrigerator for the Micro-X Sounding Rocket Telescope," *Adv. in Cryogenic Engineering*, Vol. 55, Amer. Institute of Physics, Melville, NY (2010), pp. 633-640.

14. Wikus, P., et al., “Micro-X, the TES X-ray Imaging Rocket: First Year Progress," *Applied Superconductivity* 19 (2009), pp. 553-556.